Society of Petroleum Engineers
6200 North Central Expwy.
Dallas, Texas 75206

PAPER
NUMBER SPE 6537

Analysis of the Response of Geothermal Reservoirs under Injection and Production Procedures

Marcelo J. Lippmann, Chin Fu Tsang and Paul A. Witherspoon

Lawrence Berkeley Laboratory
University of California
Berkeley, California 94720

Abstract

A major problem facing geothermal operations is the disposal of large quantities of relatively cool waste geothermal waters. Environmental regulations may require reinjection into the reservoir. Since the reservoir is thus cooled around the injection wells, there is some reluctance to reinject into wells that might be used for future production.

In this paper the response of a liquid-dominated geothermal reservoir to injection and production from a single well is studied. Different injection-production schemes are analyzed to explore how to minimize temporary cooling around the injection well and to optimize thermal recovery. The pressure response is also calculated, and found to be affected significantly by temperature-dependent viscosity variations. This will have implications on well-test methods for geothermal reservoirs. Vertical consolidation of the geothermal system during fluid withdrawal is also discussed, showing the need to establish previous stress history before attempting to predict the reservoir deformation.

The transport of heat and fluid through a porous reservoir is computed using a numerical model developed at the Lawrence Berkeley Laboratory. The one-dimensional consolidation theory of Terzaghi has been coupled to the heat and fluid flow to calculate reservoir compaction. No attempt is made to model chemical reactions or precipitation that might occur when waters of a different temperature and salinity are injected into the reservoir.

References and Illustrations at end of paper.

A. Introduction

A major problem facing geothermal energy development is the disposal of large quantities of relatively cool waste geothermal waters. Operators are reluctant to reinject these fluids as they could irreversibly cool the reservoir around the injection wells and affect nearby producing wells.

Gringarten and Sauty[1] used a two-dimensional semianalytical model to investigate the effect of reinjection wells on neighboring producing wells. Tsang and Witherspoon[2] used the same model to suggest the screening effect that may be found in a multiple-well system. However, this model assumes a steady fluid-flow field, neglects gravity and, even more important, ignores the dependence of parameters (such as viscosity and density) on temperature variations. Thus a detailed understanding of the behavior of a geothermal reservoir cannot be expected with this semianalytic approach.

Realistic two- or three-dimensional numerical models have been developed to analyze liquid-dominated geothermal systems (Mercer and Pinder[3]; Pritchett et al.[4]; Sorey[5], and others). To date,

no one has applied these models to the response of geothermal systems under different injection-production schemes. This paper is such an attempt. Using a numerical model (called "CCC") developed at the Lawrence Berkeley Laboratory, detailed thermal and fluid-flow calculations are made for a radially symmetric liquid-dominated system. Emphasis is placed on understanding the following problems:

a. Temperature recovery of a producing well after reinjection of cool fluid. The well is assumed to be used for injection for one year, after which it is changed into a production well with or without a shut in period in between. The effect of using a fully or partially penetrating well is also analyzed.

b. Consolidation of the reservoir, caprock and bedrock during pumping. The effect of assuming different previous stress histories (i.e., preconsolidation values) on the deformation of the system is studied.

c. Viscosity effects on transient reservoir pressure response. An analysis is made of the pressure changes resulting from a production-injection-production operation. The study of the type of pressure response observed may lead to the development of new well-test methods to establish the thermal as well as hydraulic parameters of a geothermal system.

The first two sections will describe the governing equations and the computer program used in the calculations. The results will then be presented and discussed, followed by summary and conclusion.

B. Governing Equations

Several authors have developed the equations governing the heat and mass flow through porous media, based on the principle of conservation of mass, momentum and energy (Mercer er al.[6]; Pritchett et al.[4]; Witherspoon et al.[7], and others).

In our studies, we are interested in a slightly-compressible liquid-dominated geothermal system. In this case, the equations of heat and mass flow through a saturated deforming porous media may be expressed in integral form as,

$$\frac{\partial}{\partial t}\int_V (\rho c)_M T dV = \int_S K_M \nabla T \cdot \bar{n} dS - \int_S \rho c_F \delta T \bar{v}_d \cdot \bar{n} dS + \int_V q dV \quad (1)$$

$$\frac{\partial}{\partial t}\int_V \frac{\rho}{1+e}\left(e\kappa + \frac{de}{d\sigma'}\right) P\, dV = \int_S \frac{k\rho}{\mu}(\nabla P - \rho\bar{g}) \cdot \bar{n} dS + \int_V Q dV \quad (2)$$

For a definition of the symbols the reader is referred to the Nomenclature.

A comment needs to be made on the capacity term on the left-hand-side of the mass flow equation (Eq. 2). This term, as shown, includes the compression of the water (κ) and the compression of the rock/soil skeleton ($de/d\sigma'$). In hydrogeology it is more customary to write the left side of Eq. 2 as

$$\frac{\partial}{\partial t}\int_V \frac{S_s}{g} P dV ,$$

where S_s, coefficient of specific storage, is usually considered to be a constant.

In most examples presented here a constant value of S_s is used, implying an elastic response of the rock skeleton to pore pressure changes. But in the cases illustrating the compaction of the system, the form given in Eq. 2 is used, implying a response partly elastic and partly non-elastic. According to the one-dimensional consolidation model of Terzaghi[8], the void ratio (e) of a material, which is a ratio of the void to solid volumes, is a function of its present effective stress (σ') and its previous stress history. Further details on how void ratio changes with effective stress (i.e., $de/d\sigma'$) will be discussed in a later section. Because of the one-dimensional nature of Terzaghi's model vertical displacements result from the void ratio changes. These deformations are restricted to the saturated formations which release water from storage during the fluid withdrawal. These vertical displacements may or may not be reflected at the ground surface as land subsidence. The external loading of the overburden, caused by the deformation of the deeper saturated formations may result in displacements at the surface that may be quite different in magnitude and direction.

The governing equations (Eqs. 1 and 2) are non-linear and are interconnected by,

a. the second order equation of state for the fluid, $\rho = \rho_o[1 - \beta(T - T_o) - \gamma(T - T_o)^2]$,

b. the Darcy velocity ($\bar{v}_d$) used in the convection term of the energy equation (Eq. 1) and

c. the temperature and/or pressure dependence of some parameters.

C. Numerical Model "CCC"

The numerical model "CCC" (for Conduction-Convection-Consolidation) developed at the Lawrence Berkeley Laboratory is used to solve numerically the heat and mass flow equations and to compute the one-dimensional consolidation of the simulated systems. This program which is a modification of program SCHAFF[5] and TRUST[9],

employs an Integrated Finite Difference Method[10] using and explicit-implicit iterative procedure to advance in time. Details of the algorithms are given by Edwards[11], Narasimhan[9] and Sorey[5]. In finite difference form the energy and mass flow equations (Eqs. 1 and 2) are given respectively by,

$$\left[(\rho c)_M V\right]_n \frac{\Delta T_n}{\Delta t} = \sum_m \left[(K_M A)_{n,m}\left(\frac{T_m - T_n}{d_{n,m}+d_{m,n}}\right) + \left(\rho c_F v_d A\right)_{n,m}\left(T_{m,n} - T_n\right)\right] + (qV)_n \quad (3)$$

$$\left[\frac{\rho}{1+e}\left(e\kappa + \frac{\Delta e}{\Delta \sigma'}\right) V\right]_n \frac{\Delta P_n}{\Delta t} = \sum_m \left[\left(\frac{k\rho A}{\mu}\right)_{n,m}\left(\frac{P_m - P_n}{d_{n,m}+d_{m,n}}\right) - \left(\frac{k\rho^2 \eta}{\mu} A\right)_{n,m} g\right] + (QV)_n \quad (4)$$

The definitions of the distance $d_{n,m}$ and the area $A_{n,m}$ in the above equations are illustrated in Fig. 1.

The coupled Eqs. 3 and 4 are solved alternatively by interlacing them in time; this is shown schematically in Fig. 2. The flow equation solves for P, $\bar{v}_d$ and e assuming that the temperature dependent properties remain constant. Then the energy equation computes T assuming that $\bar{v}_d$ and pressure dependent properties remain constant. Since the pressure varies much faster than the temperature, much smaller time steps have to be taken in the flow cycles than in the energy cycles (Fig. 2) in order to compute pressure variations accurately.

Program "CCC" is designed to simulate one-, two- or three-dimensional heterogeneous isotropic, non-isothermal saturated porous systems. Thermal and hydraulic properties may be temperature and/or pressure dependent; deformation parameters may be non-linear and non-elastic. The following physical effects relevant to fluid injection-production operations can be modeled using this code:

a. Heat convection and conduction within and between the reservoir, caprock and bedrock;

b. Flow of waters of different temperatures;

c. Regional groundwater flow;

d. Spatial variation of rock properties (heterogeneity);

e. Temperature and pressure dependence of rock and fluid properties;

f. Vertical compaction of saturated formations;

g. Different production and injection schemes (number of wells, rates, temperature of injected waters).

The program has been validated against different analytical and semianalytical solutions[12].

D. Study of Temperature Recovery of a Geothermal Production Well after an Injection Period

A number of examples are given below to illustrate the effects of different injection and production schemes on the reservoir temperature distribution when one well is used first as an injector and later as a producer. In some cases a fully penetrating well is considered, while in others, a partially penetrating one. In most instances pumping immediately follows a 360-day injection period, in a few other cases the system is shut in for 360 days between injection and production.

The simulated geothermal system consists of a reservoir, a caprock and a bedrock, each 100 m thick. The caprock and bedrock are of the same type of material, while the reservoir is of a different type (see Table 1). The water is assumed to be pure, its properties are given in Table 2. The system is axisymmetric, its initial temperature and pressure conditions are given on Fig. 3. The boundary conditions are as follows:

a. the top and lower boundaries are impermeable and isothermal (235° and 265°C, respectively),

b. the radial boundary at a distance of 380 m is a constant-pressure-and-temperature boundary for the aquifer and a closed boundary for the caprock and bedrock,

c. the well located at the center of the system is pumped and injected at a constant total rate of 2.5×10^6 kg/day. The temperature of the injected water is 100°C.

In all cases it is assumed that the intrinsic permeability (k), thermal conductivity (K_M) and heat capacity of the rock as well as the compressibility (κ) and coefficients of thermal expansion (β, γ) of the water are constant. The fluid density (ρ), heat capacity (c_F) and viscosity (μ) are temperature dependent. The mesh used in these examples is illustrated on Fig. 4.

Example D-1. Fully Penetrating Well

In this example the well is injecting 2.5×10^6 kg/day of 100°C water uniformly into the 100-meter thick reservoir. After 360 days of injection (total time, t = 360 d) the temperature distribution within the aquifer is shown in Fig. 5A.

If before pumping, the well is shut in for a period of 360 days there is time for the high pressure zone around the well to dissipate. The

temperature after the shut in period (t = 720 d) is given in Fig. 5B. During the shut in period the reservoir has gained some heat from the caprock and bedrock as water forced into them during the injection period flows back into the reservoir. After the shut in, production starts at the same constant rate (2.5×10^6 kg/day). After 360 days of production (t = 1,080 d) the temperature distribution is shown in Fig. 5C. Some of the cold water still remains in the reservoir. As a function of production time the temperature of the produced water is slowly increasing, approaching assymptotically the original average reservoir temperature (250°C)(Fig. 6, curve a). If instead of shutting in the well, pumping is started immediately after the injection period (t = 360 d) the temperature distribution after 360 days of production (t = 720 d) is found not to differ significantly from that given on Fig. 5C. This is also indicated by the temperature of the produced waters (Fig. 6, curve c).

Example D-2. Partially Penetrating Well. Injection and production from the upper part of the reservoir.

In this case, the well injects into and produces from the upper 40 m of the reservoir, at the same rate as in the previous example. The temperature profile after 360 days of injection is given on Fig. 7A. It shows that the cold water has travelled farther into the upper part of the aquifer, and less into the lower part, than in the full penetration case.

After 360 days of shut in (t = 720d) the temperature distribution (Fig 7B) reflects the effect of the colder (and heavier) water sinking and mixing with the hotter water below. Fig. 7C shows the temperature after 360 days of production from the top 40 m of the reservoir (t = 1,080 d). The temperature of the produced water is given in Fig. 6, curve b. Clearly in this case the temperature recovery is similar to that of the fully penetrating well (Ex. D-1).

Example D-3. Partially Penetrating Well. Injection into the lower part, production from the upper part of the reservoir.

This example differs from the previous one in that the injection is made into the lower 40 m of the reservoir instead of its upper part. In this way the cold water is pushed along the bottom of the reservoir and its higher density and viscosity slows down its migration towards the upper regions of the system.

Fig. 8A shows the temperature distribution in the reservoir after 360 days of injection. As expected most of the cold water stays at the bottom of the reservoir. If after injection the well is shut in for 360 days, only small temperature changes are observed. The cold water is relatively immobile. Since there appears to be no advantage in shutting in the well, the case of immediate production after injection is analyzed. In this example the pumping is done from the upper 40 m of the reservoir to minimize the extraction of cold water from the bottom. The temperature distribution after 360 days of pumping (t = 720 d) is given on Fig. 8B. It indicates that the cold water is only slowly migrating towards the producing interval because of its high density and viscosity.

This scheme of injection and production at different levels results in pumped water whose temperature is always higher than that of the injected water (Fig. 6, curve d). Because the cold water is slowly pumped out of the reservoir the temperature of production, even though is higher at the beginning, does not approach the initial average reservoir temperature as fast as in the two previous cases.

Example D-4. Partially Penetrating Well. Injection into the reservoir below a low permeability lens, production from above the lens.

This case is intended to illustrate the dramatic effect of even a small lens of low permeability material on the temperature of the produced waters when injection into reservoir is done below the lens and production is from above it. The only difference between this case and example D-3 is that a 20 m-thick, 25 m-radius lens of the same material as the caprock is present at the center of the system (Fig. 9).

After 360 days of injection below the lens the temperature in the reservoir is shown in Fig. 9A. The lens has greatly restrained the flow of cold water towards the upper part of the system. The injected water has moved along the bottom of the reservoir farther away from the well than in any of the cases considered before.

As in the previous example no advantage is expected from shutting in the system after injection. Therefore, production from above the lens is started immediately after the injection period. The temperature in the reservoir after 360 days of pumping (t = 720 d) is shown on Fig. 9B. The temperature in the upper part of the system is higher than in example D-3, the upward movement of the colder water is slowed down not only by its high density and viscosity but also by the presence of the low permeability lens. This is reflected by the temperature of the produced water (Fig. 6, curve e). The temperature drops slightly at the beginning, then stabilizes, and finally slowly rises after three months of production. It never drops below 210°C.

Remarks

These examples illustrate the importance of planning an injection operation if the wells are intended to be used later for production. The

colder waste waters should be injected into the lower part of the geothermal reservoir and production should be made from the upper part. This will take advantage of the water density and viscosity variations with temperature. Most of the cold water which is denser and more viscous than the warmer geothermal water will tend to remain at the bottom of the reservoir. When production starts from the top, the warmer water will tend to move radially towards the well without large-scale mixing with the cold water from below. Example D-4 illustrates the important effect of an heterogeneity in the reservoir. Even a small lens of 25 meter radius greatly affects the temperature of the produced water, if injection is done below it and pumping from above it. The ultimate case would be a continuous layer of low permeability (aquitard) dividing the reservoir into two parts. In this case, the temperature of the upper region will not be affected appreciably if cold water is injected into the lower part. But in this case no major recharge of the upper system will occur, resulting in larger pressure drops. From Fig. 6 it may be concluded that a well which has been used for reinjection will eventually regain its initial temperature. Its rate of recovery will depend on how the reinjection of cold water was made. If some initial drop of temperature does not affect its intended use, the produced water may be used immediately assuming that the injection is made into the bottom followed by production from the top of the reservoir (Fig. 6, curves d and e). If an appreciable temperature change cannot be tolerated, at the beginning some of the pumped water will not be adequate, but after a period of time the temperature of the water will approach its initial value. In this case a fully penetrating well will result in a faster recovery (Fig. 6, curve c). It has been shown that shutting in the well between injection and production periods will not greatly affect the temperature of the produced water.

The results presented here may have been different if regional flow is present across the system. If one considers only one well, the regional flow, if it is of hot water as it should be in a geothermal field, will accelerate the recovery of the well because it will sweep the injected waters away from the well.

Several simplifying assumptions were made which might affect the conclusions given above:

a. No precipitation of salts or chemical reactions were considered. The injection of waters of different physical and chemical characteristics into a hot geothermal reservoir may produce some reactions between the waters and rocks which may change the hydraulic properties of the formation.

b. All waters were assumed to be pure. In general, geothermal waters have high salinities; the characteristics of the injected waters may be different from those of the geothermal waters. The properties of these waters, especially viscosity and density, will differ somewhat from those of pure water.

c. The rocks were assumed to be isotropic. In general, rocks present some anisotropy especially in their permeability. In most cases, the horizontal permeability is larger than the vertical. This will enhance the horizontal flow of fluids and reduce their vertical flow. The lens of low permeability intercalated in the reservoir shown in Example D-4 has a similar effect.

E. Study of Consolidation During Fluid Production

Several cases were studied to obtain some insight on how to minimize compaction resulting from successive injection and production operations. It was found that the deformation of the system depended heavily on the properties assigned to the different materials. If the same properties were used similar results were obtained when totally or partially penetrating wells were modeled. Rebound accompanied injection, but a final net compaction resulted from pumping, because of the partial non-elastic response of the materials to changes in effective stress (i.e., total stress minus pore-pressure).

In the model used, the consoldation behavior of each material is described by "e-log σ' curves" (Fig 10). There is a so-called virgin curve and a series of parallel swelling-recompression curves (the model neglects the hysteresis between swelling and recompression curves). When the rock (soil) is loaded to levels never reached before, its deformation is given by the virgin curve, of slope C_c. As the effective stress (σ') increases, the void ratio (e) of the material decreases. When σ' decreases, the changes in e are not given by the virgin curve, but by swelling curves of slope C_s. Generally C_s is one order of magnitude smaller than C_c. If σ' is first decreased and then increased, the reduction in void ratio is given by the same curve (now called recompression curve) until the effective stress reaches its previous highest value (preconsolidation stress). At that point the system starts to follow the virgin curve again This means that the deformation of the system is dependent on its previous stress history.

When the effective stress of a material is equal to its preconsolidation stress it is said tc be normally consolidated (its void ratio is given by the virgin curve). If the preconsolidation stress is greater than the effective stress, the material is said to be overconsolidated (its void ratio is given by one of the swelling-recompression curves).

In a previous paper[13] the compaction of liquid-dominated geothermal systems has been illustrated. Here, the need to establish the previous stress history (i.e., preconsolidation stresses) of a system before attempting to predict its compaction behavior will be emphasized. The vertical deformation and pressure changes vary significantly when different preconsolidation values are assumed. The preconsolidation stress determines whether a material follows the virgin or a recompression curve when pumping occurs. In the case of injection (i.e., reduction of effective stress) the material always behaves according to one of the swelling curves.

The system analyzed is the same as in the previous section, the only difference is that the deformation of the rock skeleton is given by "e-log σ' curves". Table 3 lists the deformation parameters used in the calculations. The overburden (not shown on Fig. 2) is assumed to be 450 m thick and its average density, 2,500 kg/m^3. The well is fully penetrating the reservoir and is pumping at a rate of 2.5 x 10^6 kg/day for a 30-day period.

Example E-1. Overconsolidated Materials. Overconsolidation: 7 x 10^5 N/m^2.

In this example, because of the high overconsolidation of the materials (preconsolidation-effective stress = 7 x 10^5 N/m^2), the deformation behavior of the system is given by the recompression curves. The deformation of the 300-m thick system is relatively small (Fig. 11, curve a). Little water is obtained from the compression of the rock skeleton. This is reflected by a rapid decrease in pore pressure in the reservoir (Fig. 12A, curve a). The rapid stabilization of the pressure is mainly the results of the constant pressure condition assumed at the outer boundary of the system. The compaction of the reservoir is significant at the beginning of the pumping period but later that of the caprock and bedrock becomes much more important[13]. The consolidation of the system continues even after the pressure has stabilized in the reservoir, because the pressure in the caprock and bedrock continues to decrease (Fig. 13).

Example E-2. Normally Consolidated Materials. Overconsolidation = 0.

Because of their normal consolidation during all the pumping period the materials deform according to their virgin curves. Considerable consolidation occurs (Fig. 11, curve c), releasing larger amounts of water than in the previous case. This is reflected by a much slower reduction in pore pressure (Fig. 12A, curve c).

Example E-3. Overconsolidated Materials. Overconsolidation = 2 x 10^5 N/m^2.

This case is intermediate to the two previous examples. At the beginning the system deforms according to the recompression curves. After the point where the effective stress increase (i.e., pore pressure decrease) is equal to the overconsolidation value, the reduction of void ratio follows the virgin curves. This intermediate behavior is reflected in the pressure and deformation of this system (Figs. 11 and 12, curves b).

Remarks

Figs. 11 and 12 illustrate the consolidation and pressure behavior of a geothermal system when different previous stress conditions are assumed. For comparison purposes, these figures also show the pressure changes obtained when a totally elastic behavior of the material is assumed, as it is normally done in hydrogeology and petroleum engineering. (The coefficients of specific storage used in this particular calculation are given on Table 1.)

The different pressure response to pumping is emphasized when reservoir pressure is plotted against the reciprocal of time (Fig. 12B). The difference in curvature shown by the graphs may help to establish the deformation properties of a given system under production.

Fig. 14 shows the changes of pore pressure versus consolidation. This graph clearly reflects the effects of differences in overconsolidation stresses and in the slopes of the virgin and recompression curves. The flattening out of the curves at the top is related to the constant pressure boundary used in the model.

The behavior of the system with an overconsolidation equal to 2 x 10^5 N/m^2 (Fig. 14, curve b) is very instructive. At the beginning it is identical to that of the system with a higher overconsolidation (curve a). When the pressure drop is equal to the overconsolidation value, the behavior is similar to that of the normally consolidated system (curve c). At that stage, curves b and c are essentially parallel. This response to production is similar to that observed in the Wairakei geothermal field as shown in Fig. 15, taken from Pritchett et al[14].

Soil mechanics laboratory techniques are available to measure the overconsolidation and deformation properties of materials[15]. Field tests may establish the total stress[16] and fluid pressures existing at different points of the reservoir, caprock and bedrock. These methods will allow us to obtain the correct parameters so that a numerical model, like the one presented here, may be utilized to predict the compaction behavior of a particular geothermal system. At this time no general conclusions about the consolidation of geothermal systems

may be drawn from this study since the results are so dependent on material properties (and assumed boundary conditions.

F. Study of Effect of Temperature-Dependent Viscosity on Transient Pressure Response

Several authors have stressed the importance of variable viscosity on the onset of free convection in geothermal porous reservoirs[17,18]. However, they did not discuss its effect on transient well-test analysis.

In this section we will employ our model to study the transient pressure response during a production-injection-production sequence. For this analysis a 100-m thick,1,000-m radially symmetric reservoir is considered. The same initial temperature and pressure as given on Fig. 3 are used. However, in this case all boundaries of the reservoir are closed to heat and mass flow. The well flow rate and the reservoir properties are the same as before. Near the well the mesh used is much finer than the one shown on Fig. 4, with discrete radial steps Δr set to one meter.

The well is first pumped for five days (total time, t = 0-5 days); this is followed by five days of injection of 100°C water (t = 5-10 d); finally the well is pumped for another 15 days (t = 10-25 d). The pressure changes obtained at the center of the reservoir, 1.5 meters from the axis of the system is shown on Fig. 16B. The pressure decreases normally during the first pumping period (t = 0-5 d); no temperature changes are observed. During injection the pressure increases as expected (t = 5-10 d); the temperature almost immediately drops as the cold water is injected.

During the final period of production (Fig. 16B; t = 10-25 d) the pressure begins falling much faster than during the first period of pumping. Then it stabilizes to a more or less constant pressure value before continuing to decrease. The last part of the curve appears to be a continuation of the curve corresponding to the first pumping period. This response can be explained by studying the temperature and viscosity variation observed during this period (Fig. 16A). During almost the first two days of the second pumping period the temperature remains low, then it slowly increases as the hotter water replaces the cold water being produced at the well. On the other hand, the viscosity of the fluid is high at the beginning and then rapidly decreases as the temperature rises.

For the same flow rate, the higher initial values of viscosity result in larger pressure decreases. As the temperature increases, and the viscosity decreases, the pressure stabilizes and then finally begins to drop again as a more or less constant temperature is attained. After about eight days the temperature in the reservoir is similar to that prevailing during the initial pumping period (t = 0-5 d). This explains why for later times the pressure curve for the second production period is almost a continuation of the dashed curve corresponding to the initial period of production (Fig. 16B).

If we assume that the pressure during the initial pumping period (t = 0-5 d) to be observed pressures during a normal well test, we can perform a typical constant-temperature Theis well-test analysis. We find that we reproduce the reservoir parameters correctly so long as we use the density and viscosity constant corresponding to the average reservoir temperature. This justifies to a certain extent the application of usual pumping well-test methods to geothermal systems.

On the other hand, as discussed above, a very interesting pressure response curve is found when the well is pumped after a period of injection of colder water. This opens the possibility of using injection-production well tests to establish some of the thermal properties of the reservoir. We are in the process of making such a study.

G. Conclusions

In this paper we have employed a validated numerical model to study temperature, pressure and consolidation behavior of a geothermal reservoir under different injection-production schemes. The capability of this program to simulate the response of liquid-dominated geothermal systems under these conditions has been illustrated.

In the examples studied we have shown quantitatively the advantages of reinjection into the lower zone of the reservoir and production from the upper zone. Consolidation associated with fluid withdrawal was also explored, showing the need to establish the stress history before attempting to predict the reservoir deformation. Interesting pressure response curves are also obtained under a production-injection-production procedure, pointing to new well-test methods for geothermal reservoirs. This is the subject of one of our current investigations.

Nomenclature

A	area	L^2
C_c	slope of virgin curve in "e-log σ' plot"	
C_s	slope of swelling-recompression curve in "e-log σ' plot"	
c_F	fluid specific heat capacity at constant volume	$L^2t^{-2}T^{-1}$

$d_{n,m}$	distance between nodal point n and interface between nodes n and m	L
e	void ratio	
$\bar{g}$	acceleration due to gravity	Lt^{-2}
K_M	thermal conductivity of solid-fluid mixture	$MLt^{-3}T^{-1}$
k	intrinsic permeability	L^2
$\bar{n}$	outward unit normal on surface S	
P	fluid (pore) pressure	$ML^{-1}t^{-2}$
Q	mass injection rate per unit volume	$ML^{-3}t^{-1}$
q	energy injection rate per unit volume	$ML^{-1}t^{-3}$
S_s	coefficient of specific storage	L^{-1}
T	temperature	T
t	time	t
V	volume	L^3
$\bar{v}_d$	Darcy fluid velocity	Lt^{-1}
β	First coefficient of thermal expansion	T^{-1}
γ	Second coefficient of thermal expansion	T^{-2}
δT	difference between the mean temperature within volume element dV and that on surface element dS	T
$\eta_{n,m}$	direction cosine of the angle between the outward normal of node n and $\bar{g}$	
κ	fluid compressibility	$M^{-1}Lt^2$
μ	fluid viscosity	$ML^{-1}t^{-1}$
ρ	fluid density	ML^{-3}
$(\rho c)_M$	heat capacity per unit volume of the solid-fluid mixture	$ML^{-1}t^{-2}T^{-1}$
σ'	effective stress	$ML^{-1}t^{-2}$

subscripts

m	at node m
n	at node n
n,m	at interface between nodes n and m
o	reference quantity

Acknowledgement

This work was done with support from the U. S. Energy Research and Development Administration.

References

1. Gringarten, A. C. and Sauty, J. P., "A Theoretical Study of Heat Extraction from Aquifers with Uniform Regional Flow," J. Geophys. Res. 80, No. 35, 4956-4962, 1975.

2. Tsang, C. F. and P. A. Witherspoon, "An Investigation of Screening Geothermal Production Wells from Effects of Reinjection," Geothermal Reservoir Engineering, P. Kruger and J. J. Ramey Jr., eds., Stanford Geothermal Program Rpt. SGP-TR-12, 62-64, 1975.

3. Mercer, J. W. and G. F. Pinder, "A Finite-Element Model of Two-Dimensional, Single-Phase Heat Transport in a Porous Medium," U. S. Geol. Survey Open File Report, 75-574, 115 p., 1975.

4. Pritchett, J. W., S. K. Garg, D. H. Brownell, Jr., and H. B. Levine, "Geohydrological Environmental Effects of Geothermal Power Production, Phase I, Systems, Science and Software Report," SSS-R-75-2733, 90 p., 1975.

5. Sorey, M. L., "Numerical Modeling of Liquid Geothermal Systems," Ph.D. Thesis, Univ. of Ca., Berkeley, 65 p., 1975.

6. Mercer, J. W. , C. Faust and G. F. Pinder, "Geothermal Reservoir Simulation," Proc, Conf. Res. Devel. Geothermal Energy Resources, Pasadena Ca., Sept. 23-25, 1974, 256-267, 1974.

7. Witherspoon, P. A., S. P. Neuman, M. L. Sorey and M. J. Lippmann, "Modeling Geothermal Systems" Presented at the International Meeting on Geothermal Phenomena and Its Applications, Accademia Nazionale dei Lincei, Rome. Lawrence Berkeley Lab. reprint LBL-3263, 68 p., 1975.

8. Terzaghi, K. "Principles of Soil Mechanics, a Summary of Experimental Results of Clay and Sand," Engineering News Record,3-98, 1925.

9. Narasimhan, T. N., "A Unified Numerical Model for Saturated-Unsaturated Groundwater Flow," Ph.D. Thesis, Univ. of California, Berk.,244 p., 1975.

10. Narasimhan, T. N. and P. A. Witherspoon, "An Integrated Finite Difference Method for Analyzing Fluid Flow in Porous Media," Water Resour. Res., 12, No. 1., p. 57-64, 1976.

11. Edwards, A. L., "TRUMP: A Computer Program for Transient and Steady State Temperature Distribution in Multidimensional Systems," Lawrence Livermore Lab., Rpt. UCRL-14754, Rev. 3., 259 p., 1972.

12. Tsang, C. F., M. J. Lippmann, C. B. Goranson, and P. A. Witherspoon, "Numerical Modeling of Cyclic Storage of Hot Water in Aquifers," presented at the Symposium on Cyclic Storage of

Water in Aquifers,Fall Annual Meeting, Amer. Geophy. Union, San Francisco, Ca., Dec. 6-10,1976, Lawrence Berkeley Lab. Rpt. LBL-5929, 1976.

13. Lippmann, M. J., T. N. Narasimhan and P. A. Witherspoon, "Numerical Simulation of Reservoir Compaction in Liquid Dominated Geothermal Systems", Proc. 2nd Int'l. Symp. Land Subsidence (in press) Anaheim, Ca. Dec. 10-17, 1976, Lawrence Berkeley Lab. reprint LBL-4462, 11 p., 1977.

14. Pritchett, J. W., S. K. Garg, and D. H. Brownell, Jr., "Numerical Simulation of Production and Subsidence at Wairakei, N. Z.," presented at 2nd Workshop Geothermal Reservoir Engineering, Stanford, Ca., Dec. 1-3, 1976.

15. Lambe, T. W. and R. V. Whitman, Soil Mechanics, J. Wiley and Sons, New York, 553p., 1969.

16. Jaeger, J. C. and N. G. W. Cook, Fundamentals of Rock Mechanics, 2nd edit., Chapman and Hall, London, 585 p., 1976.

17. Kassoy, D. R. , "Heat and Mass Transfer in Models of Underdeveloped Geothermal Fields," Proc. 2nd U. N. Symp. Develop. Use Geoth. Resources, 20-29 May 1975, San Fran., Ca. Vol 3. 1707-1711, 1976.

18. Straus, J. M. and G. Schubert, "Thermal Convection of Water in a Porous Medium: Effects of Temperature- and Pressure-Dependent Thermodynamic and Transport Properties," Jour. Geophys. Res.,82 No. 2., 325-333, 1977.

TABLE 1

Material Properties of Rocks Used in the Model

	Caprock/ Bedrock	Reservoir
Heat Capacity (joule kg^{-1} $°C^{-1}$)	930	970
Density (kg m^{-3})	2,700	2,650
Thermal Conductivity (K_M) (joule $m^{-1}day^{-1}$ $°C^{-1}$)	10^5	2.5×10^5
Intrinsic Permeability (k) (m^2)	2.9×10^{-17}	2.9×10^{-14}
Specific Storage Coefficient (S_s) (m^{-1})	3.9×10^{-3}	3.9×10^{-5}
Porosity	.20	.10

TABLE 2

Fluid Properties of Water Used in the Model

Compressibility (κ)	6.5×10^{-10} m^2N^{-1}
First Coefficient of Thermal Expansion (β)	3.17×10^{-4} $°C^{-1}$
Second Coefficient of Thermal Expansion (γ)	2.56×10^{-6} $°C^{-2}$
Reference Temperature (T_o)	25°C
Reference Density (ρ_o)	997 kg m^{-3}
Viscosity (μ) and Heat Capacity (c_F)	f(T)

TABLE 3

Deformation Parameters Used in Examples E-1—E-3

	Bedrock/ Caprock	Reservoir
Reference Void Ratio (e_o)	.25	.1111
Reference Porosity	.20	.10
Reference Effective Stress (σ_o') (N/m^2)	8.71×10^6	8.71×10^6
Slope of Virgin Curve (C_c)	.5	.05
Slope of Swelling-Recompression Curve (C_s)	.01	.01

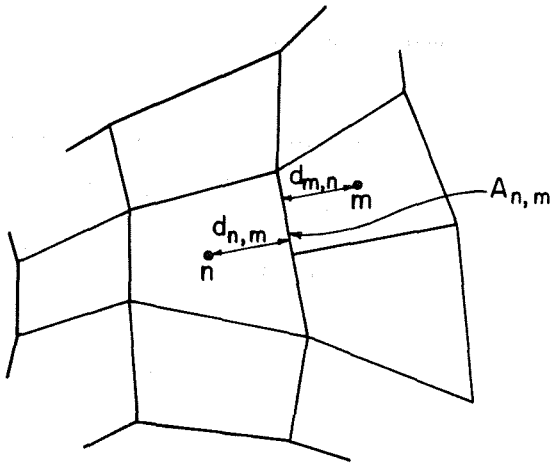

Figure 1. Typical node connection network and nomenclature.

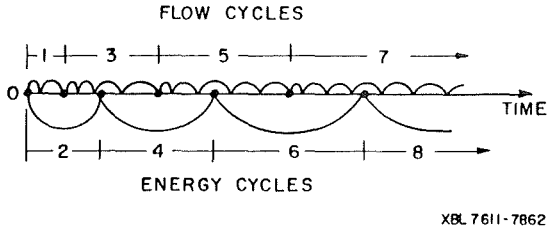

Figure 2. Interlacing of flow and energy calculations.

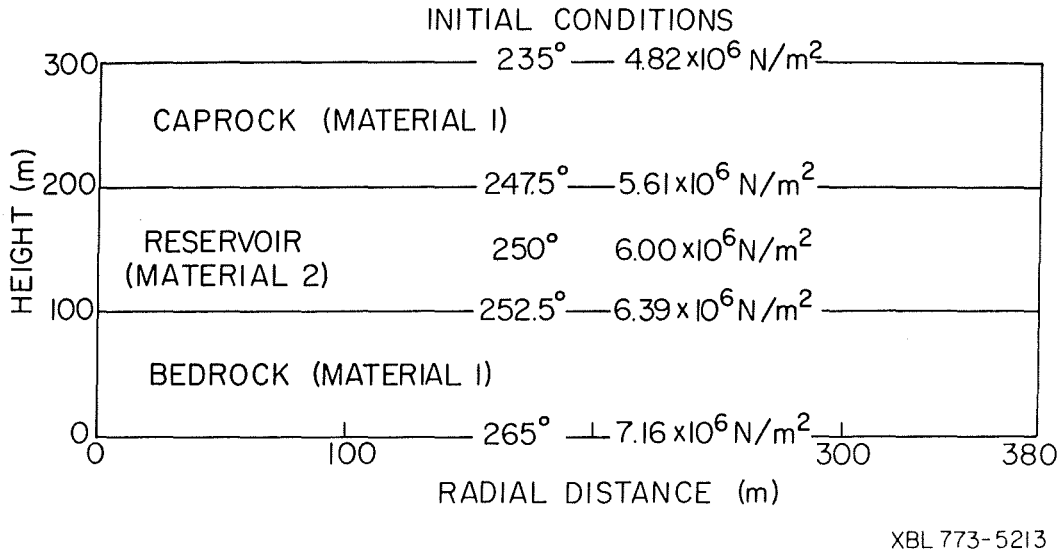

Figure 3. Geometry and initial temperature and pressure conditions of the geothermal system modeled.

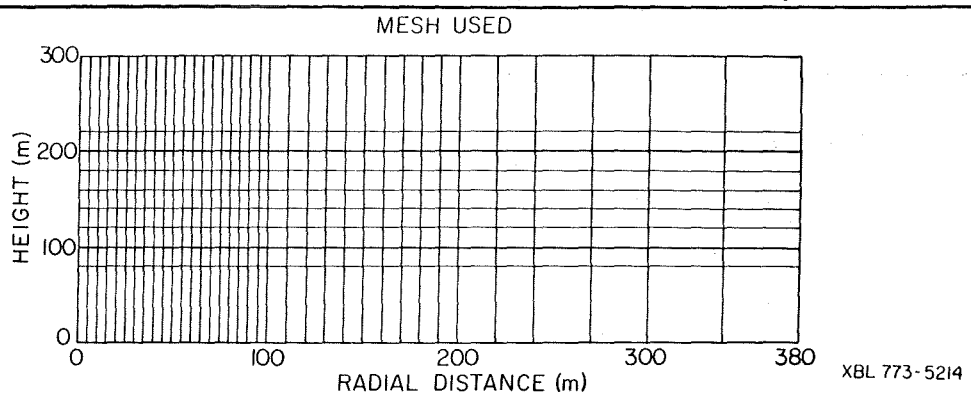

Figure 4. Mesh used in the injection-production and consolidation studies (Examples D-1 to D-4 and E-1 to E-3).

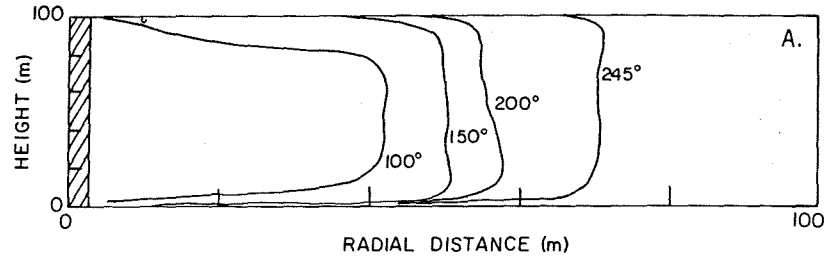

A. After 360 days of injection.

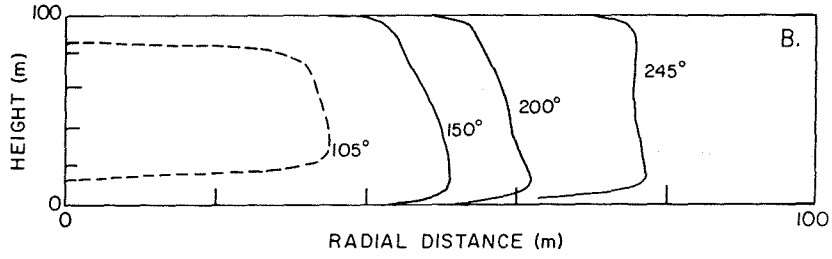

B. After 360 days of shut in (t = 720 d)

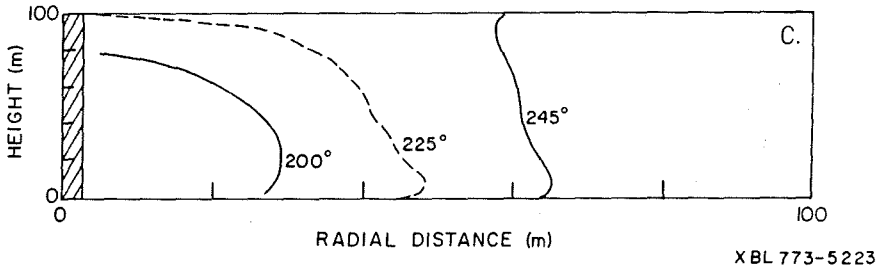

C. After 360 days of pumping (t = 1,080 d).

Figure 5. Example D-1. Temperature distribution in the reservoir. (Hatched region indicates production/injection interval.)

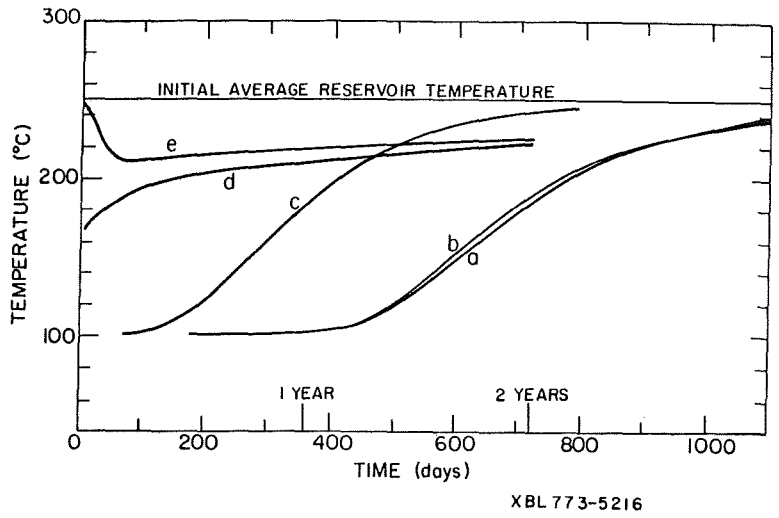

Figure 6.

Temperature of produced water. a) Example D-1: full penetration, with shut in period; b) Example D-2: injection and production at the top zone, with shut in period in between; c) Example D-1: full penetration, without shut in period; d) Example D-3: injection at bottom zone and production at top zone, without shut in period; e) Example D-4: injection below low permeability lens and production from above it, without shut in period.

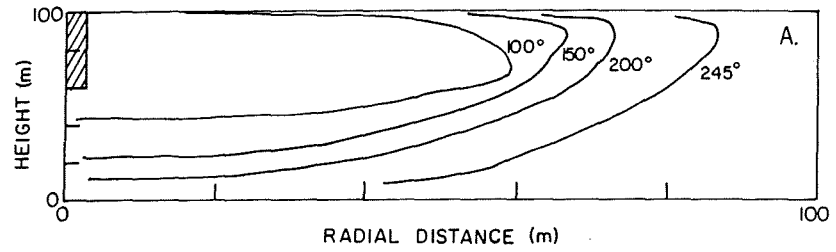

A. After 360 days of injection into the upper part of the reservoir.

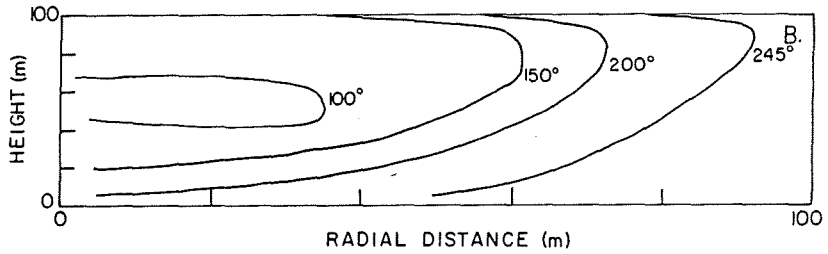

B. After 360 days of shut in (t = 720 d).

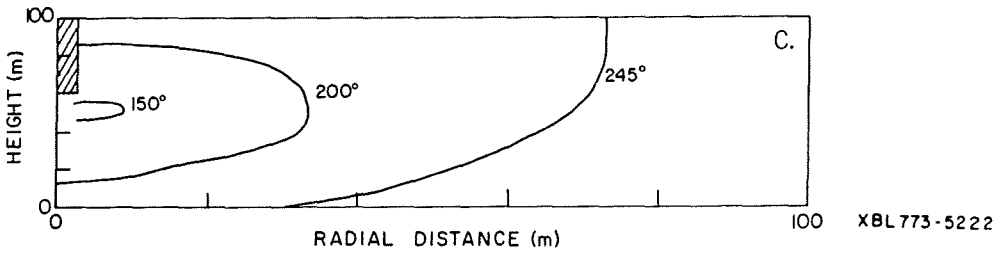

C. After 360 days of pumping from the upper part (t = 1,080 d).

Figure 7. Example D-2. Temperature distribution in the reservoir. (Hatched regions indicate production/injection intervals.)

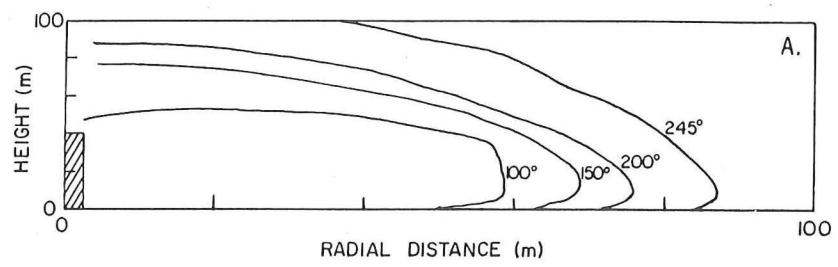

A. After 360 days of injection into the lower part of the reservoir.

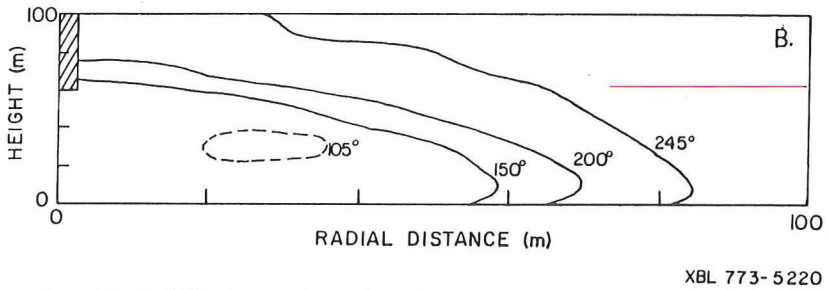

B. After 360 days of production from the upper part (t = 720 d).

Figure 8. Example D-3. Temperature distribution in the reservoir. (Hatched regions indicate production/injection intervals.)

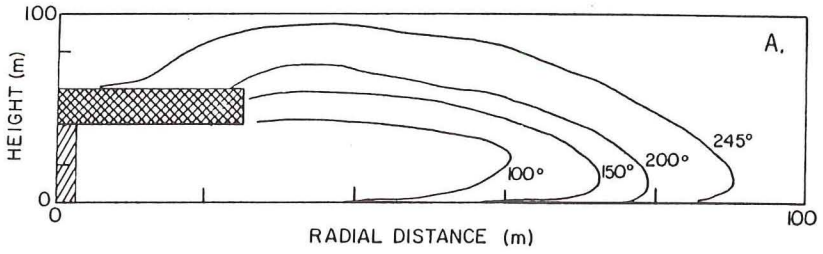

A. After 360 days of injection into the lower part of the reservoir.

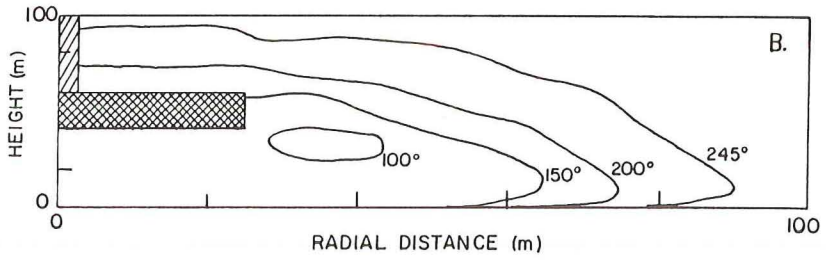

B. After 360 days of production from the upper part (t = 720 d).

Figure 9. Example D-4. Temperature distribution in the reservoir. (Hatched regions indicate production/injection intervals. Cross-hatched region represents a lens of low permeability material.)

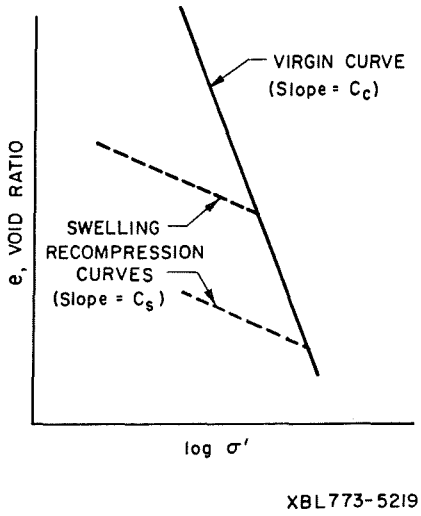

Figure 10. Plot of void ratio (e) versus effective stress (log σ') for a hypothetical material.

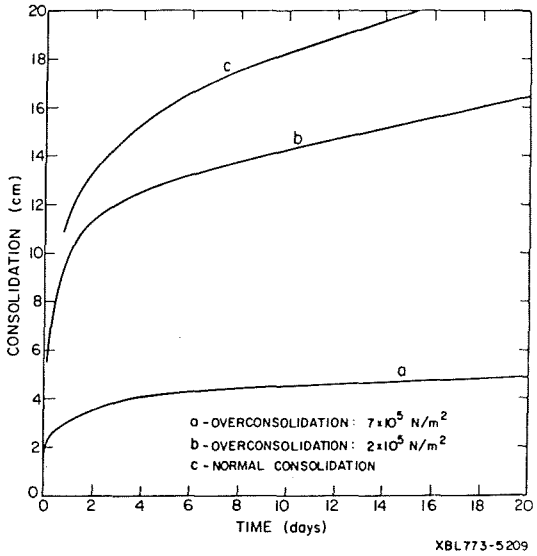

Figure 11. Plot of vertical compaction versus time under different overconsolidation conditions.

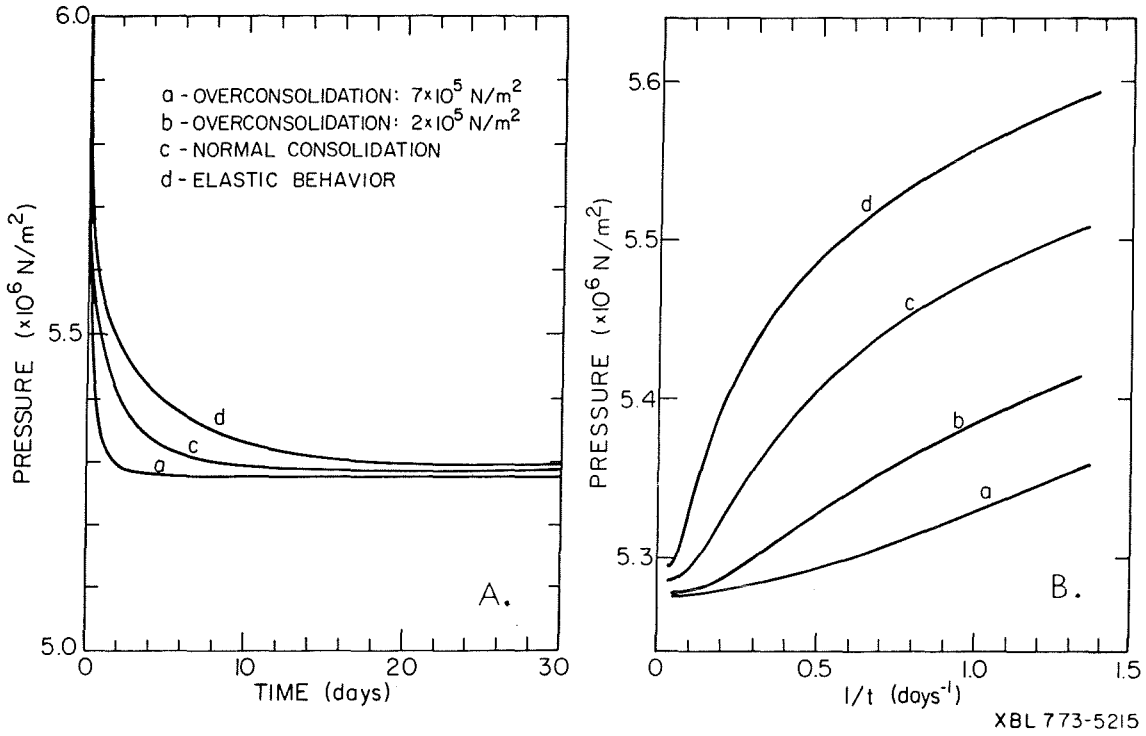

Figure 12. Plot of reservoir pressure versus: A) time, and B) reciprocal time under, different rock deformation conditions.

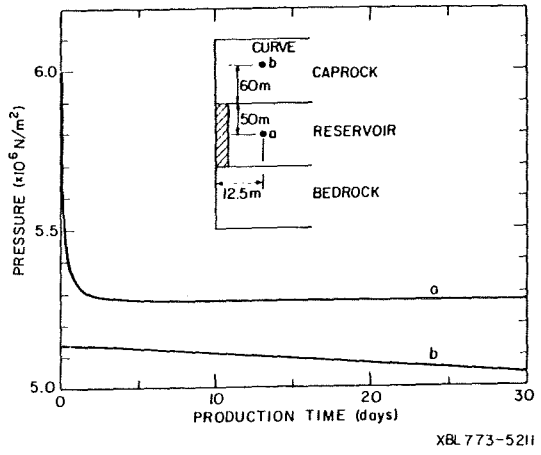

Figure 13. Example E-1. Pressure changes with time in the reservoir and caprock.

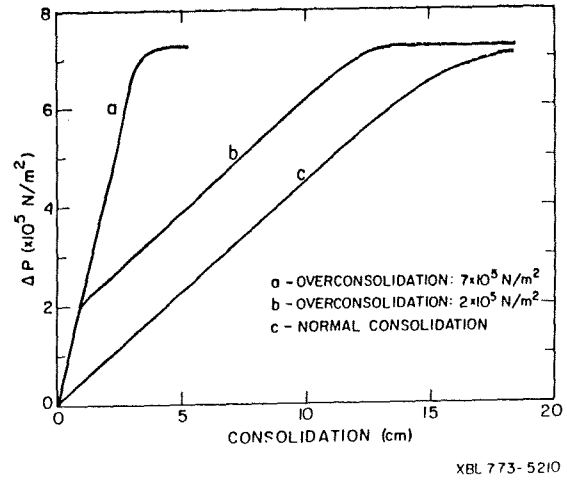

Figure 14. Plot of reservoir pressure versus consolidation under different over-consolidation conditions.

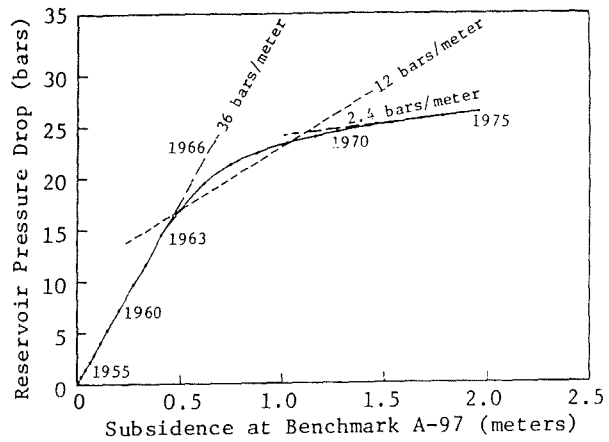

Figure 15. Reservoir pressure drop versus subsidence at Wairakei, New Zealand (taken from Pritchett et al.[14]).

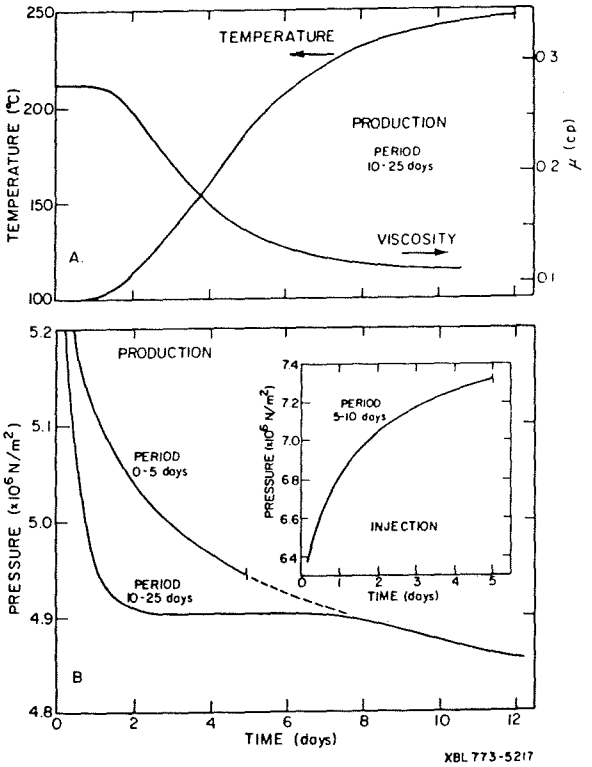

Figure 16. Effect of viscosity variation on pressure response. Plot of: A) temperature and viscosity versus time (period: 10-25 days); B) pressure versus time, for a point at the center of the reservoir, 1.5 m from the axis of the system.